Scientific Research Publishing

Applied Mathematics, 2023, 14, 1-20
https://www.scirp.org/journal/am
ISSN Online: 2152-7393
ISSN Print: 2152-7385

On the Relativistic Harmonic Oscillator

Yair Zarmi

Jacob Blaustein Institutes for Desert Research, Ben-Gurion University of the Negev, Midreshet Ben-Gurion, Israel
Email: zarmi@bgu.ac.il

How to cite this paper: Zarmi, Y. (2023) On the Relativistic Harmonic Oscillator. *Applied Mathematics*, **14**, 1-20.
https://doi.org/10.4236/am.2022.141001

Received: October 24, 2022
Accepted: January 7, 2023
Published: January 10, 2023

Abstract

The relativistic harmonic oscillator represents a unique energy-conserving oscillatory system. The detailed characteristics of the solution of this oscillator are displayed in both weak- and extreme-relativistic limits using different expansion procedures, for each limit. In the weak-relativistic limit, a Normal Form expansion is developed, which yields an approximation to the solution that is significantly better than in traditional asymptotic expansion procedures. In the extreme-relativistic limit, an expansion of the solution in terms of a small parameter that measures the proximity to the limit $(v/c) \to 1$ yields an excellent approximation for the solution throughout the whole period of oscillations. The variation of the coefficients of the Fourier expansion of the solution from the weak- to the extreme-relativistic limits is displayed.

Keywords

Relativistic Harmonic Oscillator, Weak-Relativistic Limit, Extreme-Relativistic Limit

1. Introduction

Unlike many energy-conserving oscillatory systems, the relativistic harmonic oscillator (RHO) represents a unique case. In many of these systems, the nonlinearity is a nonlinear function of the amplitude, $x(t)$. Usually, the occurrence in the nonlinearity of the velocity, $\dot{x}(t)$, represents damping and energy non-conservation. The RHO is an energy-conserving system, in which the nonlinearity involves the velocity. Furthermore, in popular systems, as the amplitude of oscillation, a, tends to infinity, the period of oscillations, T, tends to zero and the maximal velocity tends to infinity. In the case of the RHO, the period tends to infinity and the velocity tends to a constant, the speed of light, c.

The study of relativistic oscillations has progressed in several avenues: The exploitation of relativistic oscillators for the purpose of the description of bound states of quarks in High-Energy Physics [1] [2] [3] [4]; The study of the Dirac oscillator theoretically [5]-[12] and experimentally [13] [14], and the Quantum-Mechanical RHO [15]-[23]. Oscillations in the weak-relativistic limit have been of interest in Plasma Physics [24]-[36]. The emergence of chaotic behavior in a parametrically forced relativistic van der Pol oscillator is discussed in Ref. [37]. The behavior of an ensemble of RHO's is studied in Ref. [38]. Interest in the RHO, in both weak- and extreme-relativistic limits has won renewed attention in the study of media, through which light propagates at velocities that are much lower than its speed in vacuum. A recent example is that of the dynamics of an oscillator composed of ultra-cold Bose-condensed atoms [39] [40] [41], where the effective speed of light is lower than in vacuum by orders of magnitude, e.g., 143 mm/s [41]. The energy-momentum relation of the atoms is nearly identical to that of a massive relativistic particle, with an effective mass.

Over many years, the major effort in the analysis has been dedicated to either generating numerical solutions or to various approximation schemes in the weak relativistic limit by expansions in powers of β^2 ($\beta = \left(\max\left|\dot{x}\right|\right)/c$) for $\beta \ll 1$ [42]-[50]. Owing to the emergence of secular terns in asymptotic expansion methods, the validity in time of approximate solutions is limited. Typically, the lowest-order approximation ($O(\beta^2)$) in such analyses has a 1% - 2% error relative to the numerical solution up to only $\beta \approx 0.2$. One important result of Ref. [43] is the presentation the period of oscillations in the frame of reference of an outside observer in terms of complete elliptic integrals.

Qualitative progress has been attained through the exploitation of the transformation from the time variable in the observer's frame of reference to that of the oscillating mass (proper time) [51]-[57]. The oscillation period in proper time was derived in terms of a complete elliptic integral in Ref. [51]. The equivalence of the equation of motion of the RHO with a specific form of the equation of motion of a Duffing equation was found in Refs. [52] [53] [55] [57]. This has led to the derivation of a closed-from solution for the equation of the RHO in terms of Jacobi elliptic functions [51] [56].

The purpose of his paper is to expose the detailed characteristics of the solution of the equation of motion of the RHO in the weak- and extreme-relativistic limits.

Preliminary information is presented in Section 2. Exploiting the known closed-form expressions of the period, T, and the oscillation amplitude, $x_{\max}$, the time and position variables, t and x, are transformed in Section 3 into dimensionless variables, θ and η, respectively. η is (2π)-periodic in θ and bounded: $|\eta| \leq 1$. This transformation relieves the analysis in the weak-relativistic limit of the restriction on the validity in time of approximate solutions, encountered in standard asymptotic expansion perturbative analyses of the weak-relativistic limit. In addition, it naturally leads to a novel approach to the analysis of the extreme-relativistic limit.

The weak-relativistic limit is discussed in Section 4 through a Normal Form expansion [58]-[66]. As the solution is (2π)-periodic in θ, there is no need to worry about the growth of secular errors in the approximate solution for $\theta \gg 1$. A direct consequence is that the error in the approximate solution turns out to remain very small up to rather high values of β. For example, in an expansion through $O(\beta^2)$, the approximations for the dimensionless position, η, and for the velocity, η', agree with the full numerical solution within a fraction of 1% up to $\beta \approx 0.6$ and $\beta \approx 0.45$, respectively.

The expansion in powers of β^2 fails in the extreme relativistic limit ($\beta \to 1$). In this limit, over most of the period of oscillations, the velocity $\dot{x}$, oscillates between two constant values, $\pm v_{\max}$, ($v_{\max} = c\beta$) and is reduced to zero rapidly over a short time interval near the turning point. The analysis is presented in Section 5 through the introduction of a small parameter, μ, which measures the proximity to the extreme relativistic limit.

Near the turning point ($\theta = 0$), the velocity varies rapidly over a range of $O(\mu^2)$ in θ. Hence, for finding an approximate solution for η over this narrow range in the extreme-relativistic limit, a variable transformation is required, $\theta = \mu^2 z$, so that z is of $O(1)$. The resulting expansion of the solution in powers of μ^2, expected to provide a good approximation to the solution near the turning point ($\theta = O(\mu^2)$ ($z = O(1)$)), generates an excellent approximation to the solution for $0 \le \theta \le 2\pi$, even in the lowest order in μ^2, for small μ. Unique features of the Fourier expansion of the solution are discussed in Section 6. Some concluding comments are presented in Section 7.

2. Preliminaries

The dynamical equation of the RHO is:

$$m\omega_0^2 x + m\frac{\ddot{x}}{\left(1-(\dot{x}/c)^2\right)^{3/2}} = 0\,, \tag{1}$$

where m is the mass of the oscillation particle, ω_0 is the period of the oscillator in the non-relativistic limit and c is the speed of light.

The total energy is given by:

$$E = \frac{1}{2}m\omega_0^2 x^2 + \frac{mc^2}{\sqrt{1-(\dot{x}/c)^2}} = \frac{mc^2}{\sqrt{1-\beta^2}}, \quad \left(\beta = \max\left(|\dot{x}|/c\right)\right). \tag{2}$$

Solving Equation (2) for $\dot{x}$ yields the period of oscillations, T [43]:

$$T = \frac{1}{\omega_0}4\sqrt{2}\left(\sqrt{1+\frac{1}{\sqrt{1-\beta^2}}}E(k) - \left(1\Big/\sqrt{1+\frac{1}{\sqrt{1-\beta^2}}}\right)K(k)\right), \quad k^2 = \left(\frac{1-\sqrt{1-\beta^2}}{1+\sqrt{1-\beta^2}}\right). \tag{3}$$

In Equation (3), $E(k)$ and $K(k)$ are the complete elliptic integrals [67]:

$$E(k) = \int_0^{\pi/2}\sqrt{1-k^2\sin\varphi^2}\,\mathrm{d}\varphi, \quad K(k) = \int_0^{\pi/2}\left(1\Big/\sqrt{1-k^2\sin\varphi^2}\right)\mathrm{d}\varphi\,. \tag{4}$$

The maximal values of the amplitude of oscillations and of the velocity are obtained by setting $\dot{x} = 0$ and $x = 0$, respectively, in Equation (2), yielding:

$$x_{\max} = \sqrt{2}\frac{c}{\omega_0}\frac{\sqrt{1-\sqrt{1-\beta^2}}}{\left(1-\beta^2\right)^{1/4}}, \quad \dot{x}_{\max} = \beta c. \tag{5}$$

In the limit of small relativistic effects ($\beta \ll 1$), the expansion of E, T (using expansions of elliptic functions presented in [67]) and $x_{\max}$ in powers of β^2 is given by:

$$\begin{aligned}
E &= mc^2\left(1+\frac{1}{2}\beta^2+\frac{3}{8}\beta^4+\frac{5}{16}\beta^6+O\left(\beta^8\right)\right)\\
T &= \frac{2\pi}{\omega_0}\left(1+\frac{3}{16}\beta^2+\frac{129}{1024}\beta^4+\frac{1595}{16384}\beta^6+O\left(\beta^8\right)\right)\\
x_{\max} &= \frac{\beta c}{\omega_0}\left(1+\frac{3}{8}\beta^2+\frac{31}{128}\beta^4+\frac{187}{1024}\beta^6+O\left(\beta^8\right)\right)\\
\frac{x_{\max}}{T} &= \frac{\beta c}{2\pi}\left(1+\frac{3}{16}\beta^2+\frac{83}{1024}\beta^4+\frac{761}{16384}\beta^6+O\left(\beta^8\right)\right)
\end{aligned} \tag{6}$$

In the far relativistic limit ($\beta \approx 1$) it turns out to be convenient to define a new small parameter:

$$\beta^2 = 1-\mu^4, \quad (\mu \ll 1). \tag{7}$$

Equation (6) is then replaced by (the expansion of the elliptic integrals can be found in Ref. [67]):

$$\begin{aligned}
E &= \frac{mc^2}{\mu^2}\\
T &= \frac{4\sqrt{2}}{\omega_0}\frac{1}{\mu}\left(1-\mu^4\frac{3-6\log 2+4\log\mu}{16}+O\left(\mu^8\right)\right)\\
x_{\max} &= \sqrt{2}\frac{c}{\omega_0}\frac{1}{\mu}\left(1-\frac{1}{2}\mu^2-\frac{1}{8}\mu^4-\frac{1}{16}\mu^6+O\left(\mu^8\right)\right)\\
\frac{x_{\max}}{T} &= \frac{c}{4}\left(1-\frac{1}{2}\mu^2+\frac{1}{16}\mu^4\left(1-6\log 2+4\log\mu\right)\right.\\
&\quad\left.-\frac{1}{32}\mu^6\left(5-6\log 2+4\log\mu\right)+O\left(\mu^8\right)\right)
\end{aligned} \tag{8}$$

Note that both T and $x_{\max}$ tend to infinity as $E^{1/2}$.

Figure 1 shows the phase-space plot of the numerical solution of Equation (1) for a sequence of values of β. x and t are expressed in terms of dimensionless entities:

$$\tau = \omega_0 t, \quad X(\tau) = (\omega_0/c)\,x(\tau/\omega_0). \tag{9}$$

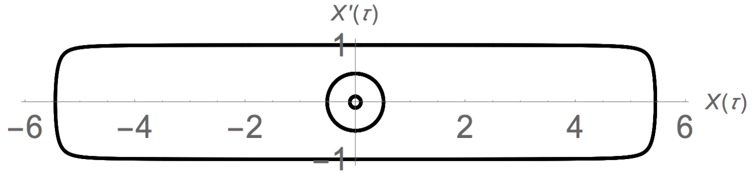

Figure 1. Phase space plots of solution of Equation (1) in terms of dimensionless entities (Equation (9)). From inner to outer plot: $\beta = 0.1, 0.5, 0.999$.

At high values of β, the phase-space plot tends to a rectangle. This has been observed in the many numerical analyse cited above.

3. Scaled Equation

Rescaling x and t as follows:

$$x(t) = x_{\max}\eta(\theta), \quad t = (T/2\pi\omega_0)\theta, \tag{10}$$

Equation (1) becomes

$$\eta(\theta) + \left(\frac{2\pi}{\omega_0 T}\right)^2 \frac{\eta''(\theta)}{\left(1 - \left(\frac{2\pi x_{\max}}{cT}\right)^2 \eta'(\theta)^2\right)^{3/2}} = 0. \tag{11}$$

$\eta(\theta)$ is (2π)-periodic in θ and bounded: $|\eta(\theta)| \le 1$. Exploiting Equations (10) and (6), yields that the maximal values of η and η' are both finite for all $0 \le \beta^2 \le 1$:

$$\begin{aligned} &\eta_{\max} \equiv \max(|\eta|) = 1 \\ &\eta'_{\max} \equiv \max|(\eta'(\theta))| = \left(\frac{\beta c T}{2\pi x_{\max}}\right) \to \begin{cases} 1 - \frac{3}{16}\beta^2 + O(\beta^4) & \beta \to 0 \\ \frac{2}{\pi} + \frac{\mu^2}{\pi} + O(\mu^4 \log \mu) & \beta \to 1 \end{cases} \end{aligned} \tag{12}$$

Figures 2-4 show the dependence of the solution on β. For $\beta \ll 1$, the phase-space plot is very close to a circle. As β is increased, it approaches a rectangle. Concurrently, η' evolves from a sine-like function of θ to a periodic step function and that of η – to a saw-tooth pattern.

For $\beta \ll 1$, Equation (11) is reduced to the equation of a classical harmonic oscillator perturbed by a small nonlinear term:

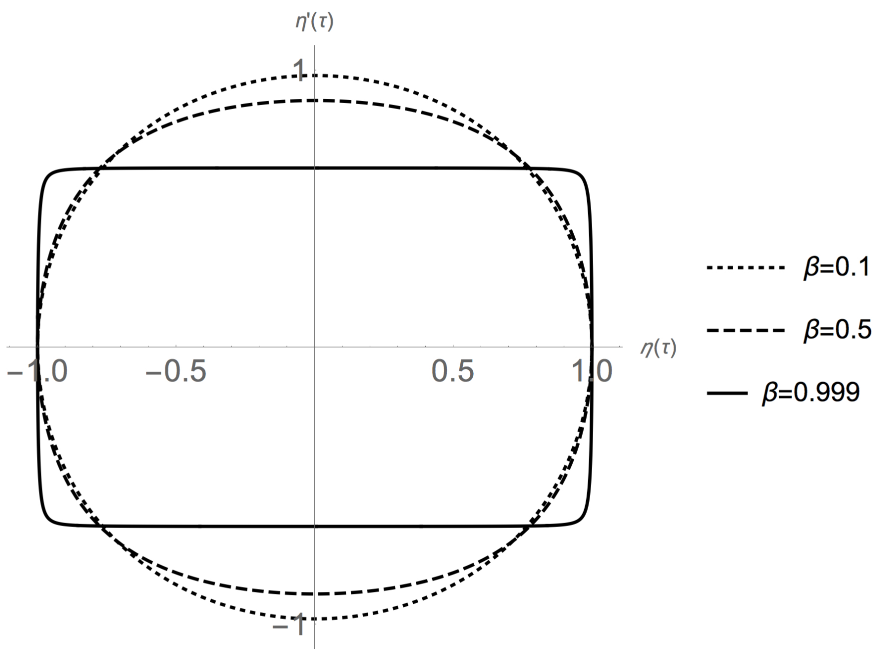

Figure 2. Phase-space plots, numerical solution of Equation (11).

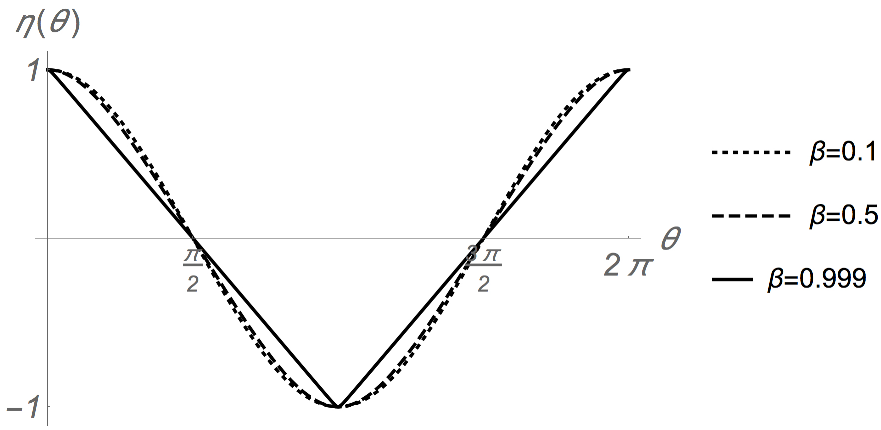

Figure 3. $\eta(\theta)$ vs. θ, numerical solution of Equation (11).

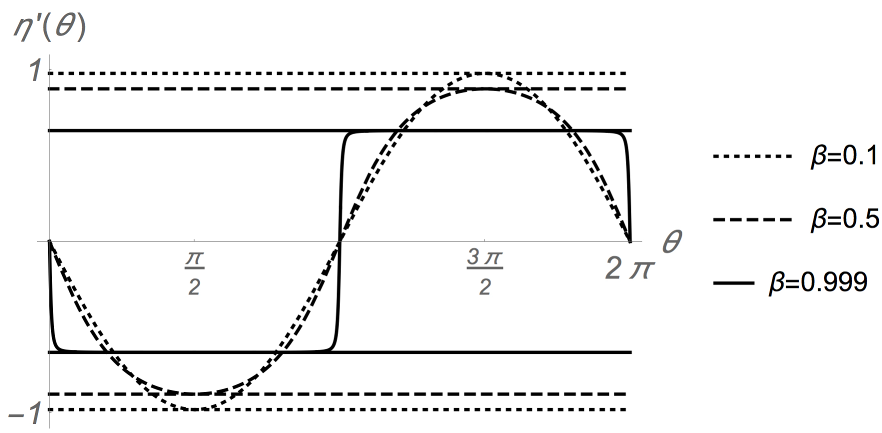

Figure 4. $\eta'(\theta)$ vs. θ, numerical solution of Equation (11). Horizontal lines are maximal values of η'.

$$\eta(\theta)+\left(1+O\left(\beta^2\right)\right)\frac{\eta''(\theta)}{\left(1-\beta^2\left(1+O\left(\beta^2\right)\right)\eta'(\theta)^2\right)^{3/2}}=0\,. \tag{13}$$

Hence, this calls for an expansion in powers of β^2.

In the extreme-relativistic limit, Equation (11), using Equations (7) and (8), and expanding in powers of $\mu \ll 1$:

$$\eta(\theta)+\frac{\pi^2}{8}\mu^2\left(1+O\left(\mu^4\log\mu\right)\right)\frac{\eta''(\theta)}{\left(1-\left(\frac{\pi^2}{4}\right)\left(1-\mu^2+O\left(\mu^4\right)\right)\eta'(\theta)^2\right)^{3/2}}=0\,. \tag{14}$$

4. Weak-Relativistic Limit

A convenient way to analyze Equation (11) is to transform it to a first-order equation for a complex entity:

$$z(\theta)=\eta(\theta)+i\eta'(\theta)\,. \tag{15}$$

Expressing η and η' in terms of z and z^*, Equation (11) is transformed into:

$$z'(\theta)=\frac{z(\theta)-z^*(\theta)}{2i} +i\left\{-\left(\frac{\omega_0 T}{2\pi}\right)^2\frac{z(\theta)+z^*(\theta)}{2}\left(1-\left(\frac{2\pi x_{\max}}{cT}\right)^2\left(\frac{z(\theta)-z^*(\theta)}{2i}\right)^2\right)^{3/2}\right\} \tag{16}$$

The boundary conditions at the turning point are:

$$\eta(0)=\frac{z(0)+z^*(0)}{2}=1,\quad \eta'(0)=\frac{z(0)-z^*(0)}{2i}=0\,. \tag{17}$$

One now writes $z(\theta)$ as:

$$z(\theta)=z_0(\theta)+\beta^2 z_2(\theta)+\beta^4 z_4(\theta)+\beta^6 z_6(\theta)+\cdots \tag{18}$$

and exploits the expansion of T and $x_{\max}$ (Equation (6)) to obtain an expansion of Equation (16) in powers of β^2.

The zero-order term of this expansion yields:

$$z_0'(\theta)=-iz_0(\theta)\Rightarrow z_0(\theta)=\rho_0 \mathrm{e}^{-i(\theta+\theta_0)}\,. \tag{19}$$

Thus, as expected, the zero-order term is (2π)-periodic in θ. The $O(\beta^2)$ term in the expansion of Equation (16) is:

$$z_2'(\theta)=-iz_2(\theta)-\frac{3}{8}i\left\{\rho_0\left(1-\rho_0^2\right)\cos(\theta+\theta_0)+\rho_0^3\cos\left(3(\theta+\theta_0)\right)\right\}. \tag{20}$$

For the solution to be periodic in θ, the coefficient of the resonant term $\cos(\theta+\theta_0)$ must vanish, yielding

$$\rho_0=1\,. \tag{21}$$

One now proceeds in the same fashion through higher orders, requiring that the higher-order corrections, z_4 and z_6 of Equation (18) are periodic in θ (*i.e.*, the coefficients of resonant terms in the dynamical equations for z_4 and z_6 vanish) and that the initial conditions are obeyed by the zero-order term:

$$\frac{z_0(0)+z_0^*(0)}{2}=1,\quad \frac{z_0(0)-z_0^*(0)}{2i}=0\,. \tag{22}$$

The result is the following expression for η:

$$\eta(\theta)=\cos\theta+\beta^2\frac{3}{64}(-\cos\theta+\cos 3\theta)+\beta^4\left(\frac{-97\cos\theta+72\cos 3\theta+25\cos 5\theta}{4096}\right) +\beta^6\left(\frac{-11619\cos\theta+6786\cos 3\theta+4000\cos 5\theta+833\cos 7\theta}{786432}\right)+O\left(\beta^8\right) \tag{23}$$

The fact that the period, T, is known explicitly means that the restriction of the validity of the approximation that emerges in well-known asymptotic expansion methods is avoided. In these methods, the period is approximated by a truncated expansion in powers of the small parameter, limiting the validity of the approximation to times of $O(1)$ or $O(1/\beta^2)$, depending on the analysis method used. This limitation is avoided here. The approximation to the full numerical solution up the rather high values of β is excellent. For β = 0.1, the maximal relative error generated by the approximate solution of Equation (23) is, at most, $O(.01\%)$. In expansions through $O(\beta^2)$, $O(\beta^4)$ and $O(\beta^6)$, the approximation for η agrees with the full numerical solution of Equation (11) within a fraction of 1% up to $\beta \approx 0.6$, 0.7 and 0.8, respectively, for all θ. The approximation for η', agrees with the full numerical solution within a fraction of 1% up to $\beta \approx 0.4$, 0.55 and 0.65, respectively, for all θ. Even for $\beta \approx 0.8$, the relative error of the approximate expression for the amplitude (through $O(\beta^6)$, Equation (23)) varies between 0 and close to 1% (see Figure 5) and for the velocity—between 1% and 5% (see Figure 6).

5. Extreme Relativistic Limit

In the extreme relativistic limit, the expansion in powers of β^2 fails. Figures 7(a)-(c) show how the approximate solution (Equation (23)) begins to deviate

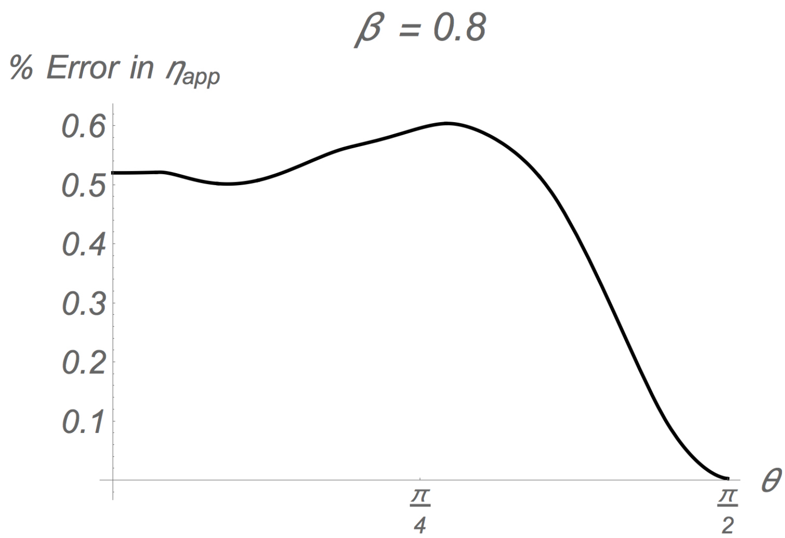

Figure 5. Error in approximate solution for $\eta(\theta)$ Equation (23) relative to numerical solution of Equation (11), $\beta = 0.8$.

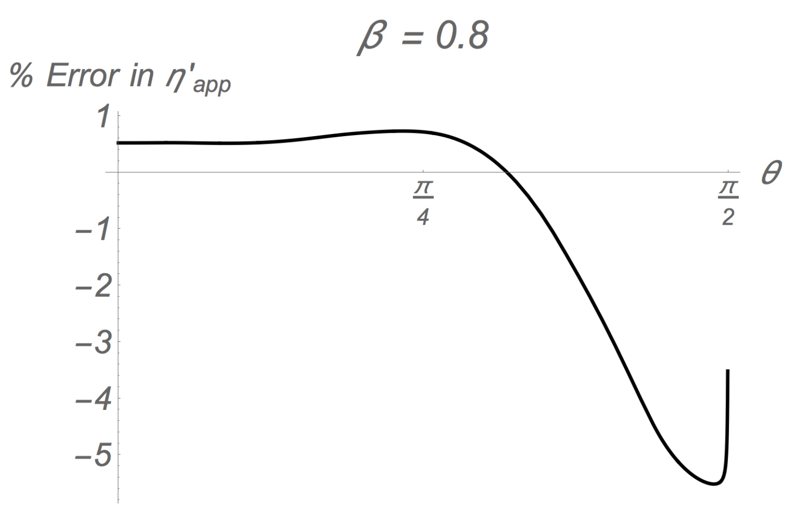

Figure 6. Error in approximate velocity $\eta'(\theta)$ computed from Equation (23) relative to numerical solution of Equation (11), $\beta = 0.8$.

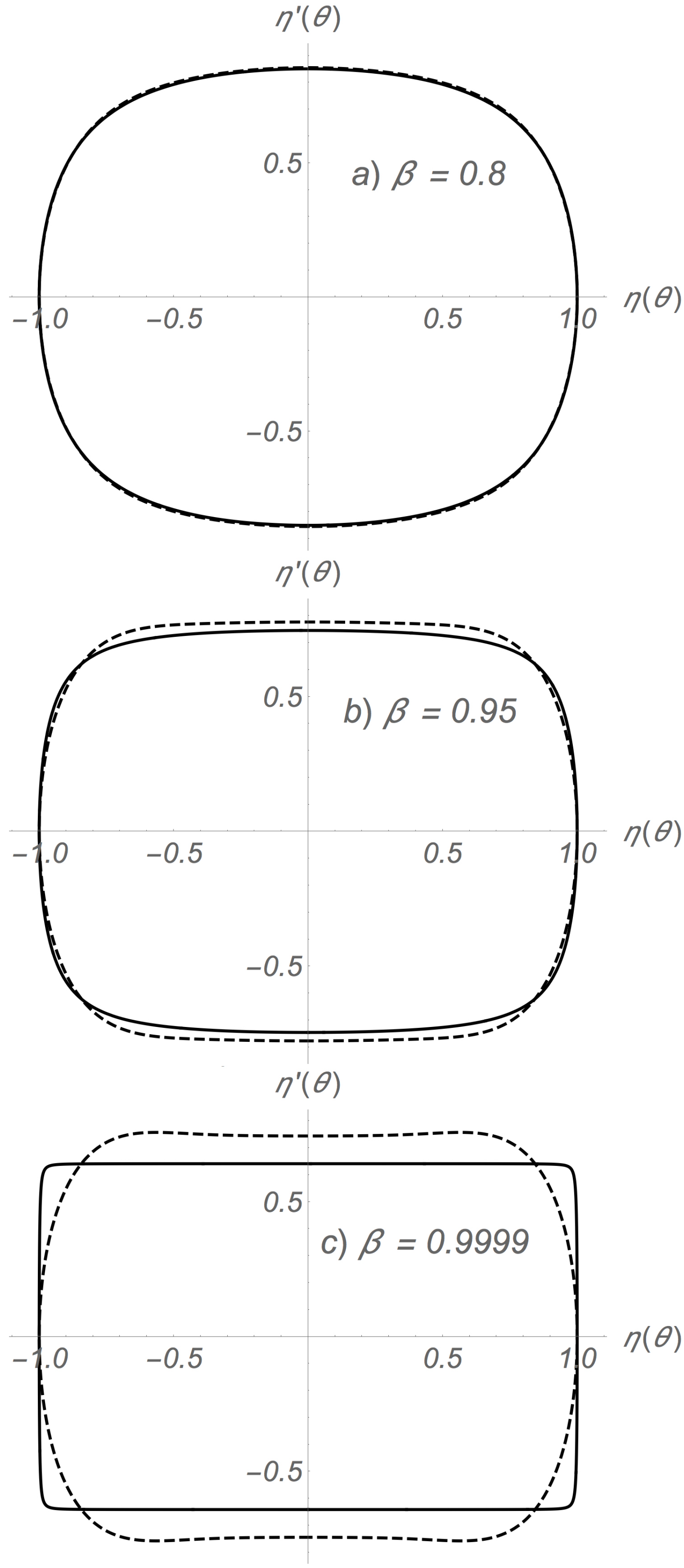

Figure 7. Phase-space plots showing evolution of deviation of approximate solution (through $O(\beta^5)$, Equation (23)) from numerical solution of Equation (11) for high β. Continuous: numerical solution; Dashed: Approximate solution.

from the numerical solution of Equation (11) as β grows. The errors in η and η' are shown in **Figure 8** and **Figure 9**, respectively, in a computation through $O(\beta^6)$, for $\beta = 0.99$. The error in η is, at most about 10%. In η', it exceeds 60% near the turning point.

In this limit, the velocity, $\dot{x}$, is constant at $(\pm c\beta)$ most of the time. It vanishes rapidly over a short time gap near the turning point (See **Figure 1**). In the scaled coordinates, the dependence of η on θ is a straight line, except very close to the turning point (see **Figure 3**).

To guide oneself towards a choice of a scaled variable that is appropriate for the analysis of Equation (11) near the turning point, one uses $\mu \ll 1$ of Equation (7), which is a measures of the proximity to the extreme-relativistic limit. Observe that η' is now very close to zero. Using Equation (8) for T and $x_{\max}$ and replacing η' by zero in Equation (14), the $O(\mu^2)$ approximation to the equation becomes:

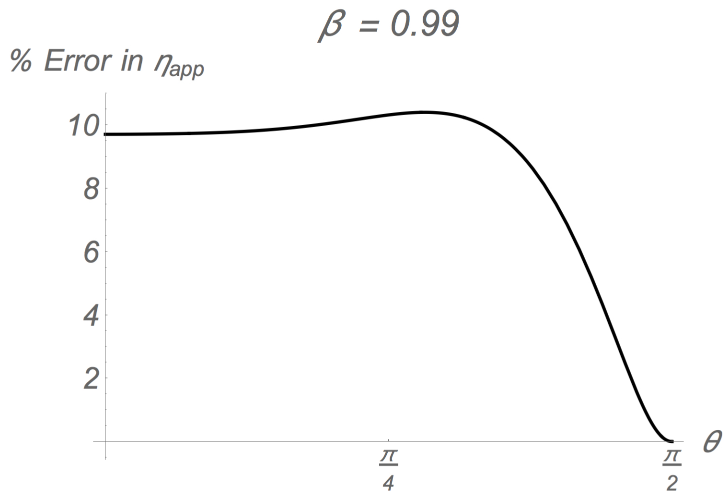

Figure 8. Error in approximate solution for $\eta(\theta)$ (Equation (23)) relative to numerical solution of Equation (11), $\beta = 0.99$.

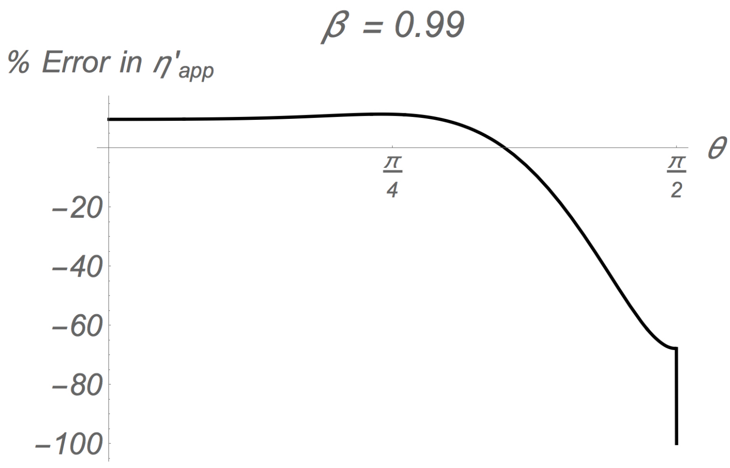

Figure 9. Error in approximate velocity $\eta'(\theta)$ computed from Equation (23) relative to numerical solution of Equation (11), $\beta = 0.99$.

$$\eta(\theta)+\frac{\pi^2}{8}\mu^2\eta''(\theta)=0. \tag{24}$$

For the boundary conditions at the turning point ($\theta = 0$), $\eta(0) = 1$ and $\eta'(0) = 0$, Equation (24) is solved by

$$\eta(\theta)=\cos\left(\frac{2\sqrt{2}}{\pi}\frac{\theta}{\mu}\right). \tag{25}$$

Exploiting the leading-order term in $\eta'_{\max}$ (Equation (12)), one finds an approximation for θ_S, the value of θ, at which the slope η' from Equation (25) becomes equal to the constant (maximal) slope that prevails throughout most of the range $0 \le \theta \le (\pi/2)$. Equation (25) yields $\theta_S = O(\mu^2)$:

$$\eta'(\theta_S)\approx-\eta'_{\max}\Rightarrow\theta_S\approx\frac{\pi}{4}\mu^2\left(1+\frac{1}{2}\mu^2\right). \tag{26}$$

Thus, for a valid expansion in powers of μ^2 near the turning point, one should rescale θ as:

$$\theta=\mu^2 z, \tag{27}$$

so that z is of $O(1)$. One now expands $\eta(\theta)$ in powers of μ^2:

$$\eta(\theta)=1+\mu^2F_2(z)+\mu^4F_4(z)+\mu^6F_6(z)+O(\mu^8),\quad \left(z=\left(\theta/\mu^2\right)\right). \tag{28}$$

Using Equations (28) and (7), one expands Equation (11) in powers of μ^2, and solves for the higher-order corrections in Equation (28). The boundary conditions for all F_{2n} are:

$$F_{2n}(z=0)=F'_{2n}(z=0)=0. \tag{29}$$

Through $O(\mu^6)$, F_{2n} are found to be given by:

$$F_2(z)=\frac{1}{2}-\frac{\sqrt{\pi^2+16z^2}}{2\pi}, \tag{30}$$

$$F_4(z)=\frac{1}{4}-\frac{\sqrt{\pi^2+16z^2}}{4\pi}+\frac{z\arcsin(4z/\pi)}{2\sqrt{\pi^2+16z^2}}, \tag{31}$$

$$\begin{aligned}F_6(z)=&\frac{1}{4}+\left(-\frac{\pi}{128}-\frac{\pi z}{8\left(\pi^2+16z^2\right)}+\frac{z}{4\sqrt{\pi^2+16z^2}}\right)\arcsin(4z/\pi)\\&-\frac{\pi^3\arcsin(4z/\pi)^2}{64\left(\pi^2+16z^2\right)^{3/2}}+\frac{\pi}{128}\log\left(\frac{4z+\sqrt{\pi^2+16z^2}}{\pi}\right)\\&+\sqrt{\pi^2+16z^2}\left(-\frac{3}{64\pi}-\frac{3\log(2)}{16\pi}+\frac{\log(\mu)}{8\pi}\right)\\&+\frac{1}{\sqrt{\pi^2+16z^2}}\left(-\frac{13\pi}{64}+\frac{13\pi}{16}\log(2)-\frac{\pi}{8}\log(\mu)\right)\end{aligned} \tag{32}$$

Detailed inspection of F_{2n} for $2n = 2, 4, 6$, reveals that they all have the same qualitative dependence on θ. Except very near the turning point ($\theta = 0$) they all tend to a linear dependence on θ. They vanish at roughly the same rate as θ varies from $O(\mu^2)$ down to zero.

The surprising result is that an expansion that was meant to be valid around the turning point ($\theta \approx O(\mu^2)$) yields an excellent approximation to the solution throughout $0 \leq \theta \leq 2\pi$ for small μ. For sufficiently small μ, an excellent approximation is obtained with just the $O(\mu^2)$ term:

$$\eta(\theta) = 1 + \mu^2 F_2(z). \tag{33}$$

Figure 10 and Figure 11 show a comparison between the approximation, Equation (33), and the numerical solution of Equation (11) for $\mu = 0.1$ ($\beta = 0.99995$). θ_S is then ≈ 0.0078. To stress the quality of the approximation, Figure 12 shows

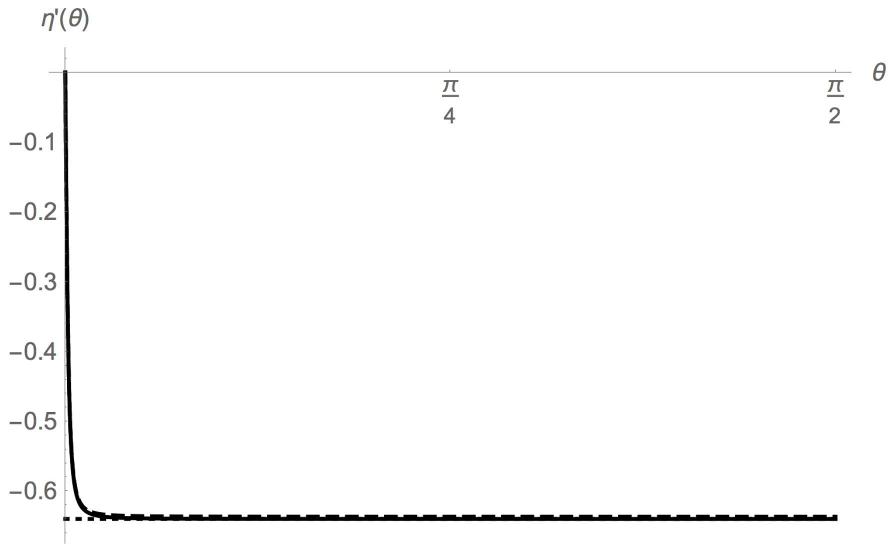

Figure 10. Comparison between the $O(\mu^2)$ approximation to the velocity, $\eta'(\theta)$ (using Equation (33), dashed) and the numerical solution of Equation (11). $\mu = 0.1$. Dotted line—constant limit of velocity beyond turning point.

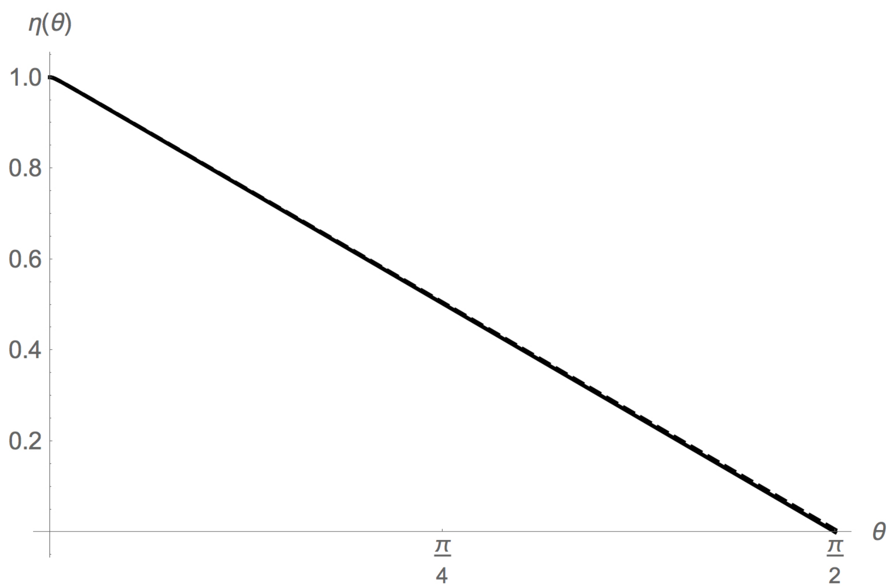

Figure 11. Comparison between $O(\mu^2)$ approximation to $\eta(\theta)$ (Equation (33), dashed) and numerical solution of Equation (11). $\mu = 0.1$.

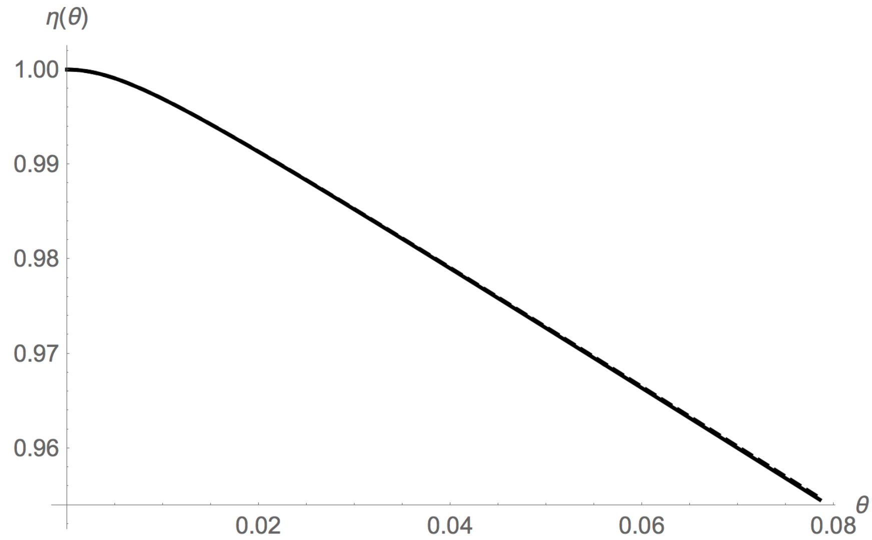

Figure 12. Comparison between the $O(\mu^2)$ approximation to the position, $\eta(\theta)$ (Equation (33), dashed) and the numerical solution of Equation (11) near the turning point. $\mu = 0.1$.

how small the deviation of the approximate solution from the numerical solution remains even for $\theta \gg \theta_S$. Figure 13 shows the relative error in η'. It remains small for all $0 \le \theta \le 2\pi$.

Finally, for $\theta = O(1)$, namely, away from the turning point, F4[$z = \theta/\mu^2$] adds a μ^2 contribution. An excellent approximation is obtained by:

$$\eta(\theta) = 1 + \frac{\mu^2}{2} - \left(\frac{2+\mu^2}{\pi}\right)\theta + O\left(\mu^4 \log\mu\right). \tag{34}$$

6. Fourier Expansion

The evolution of the velocity profile, $\eta'(\theta)$, in the extreme relativistic limit ($\beta \to 1$, $\mu \to 0$) into a periodic step function (see Figure 4) offers unique characteristics for the Fourier spectrum of $\eta'(\theta)$. The Fourier coefficients tend to the limiting spectrum of the step function, the latter oscillating between $\pm(2/\pi)$ with a cycle length of (2π). The Fourier series for this step function is:

$$\sum_{n=0}^{\infty} a_{2n+1} \sin\left(2n+1\right)\theta, \quad a_{2n+1} = -\frac{8}{\left(2n+1\right)\pi^2}. \tag{35}$$

The purpose of this Section is to discuss two aspects. The first is a demonstration of the qualitative difference between the Fourier spectra in the weak- and extremely-relativistic limits. The second is an additional test of the quality of the approximate solution obtained in Section 5.

6.1. Fourier Spectra in Weak- and Extreme-Relativistic Limits

Figure 14 presents a comparison between the β dependence of the Fourier coefficients of $\eta'(\theta)$, obtained from the numerical solution of Equation (11), and the spectrum of Equation (35). There is a qualitative difference between the β—dependence of the Fourier coefficients for small β and the spectrum of the

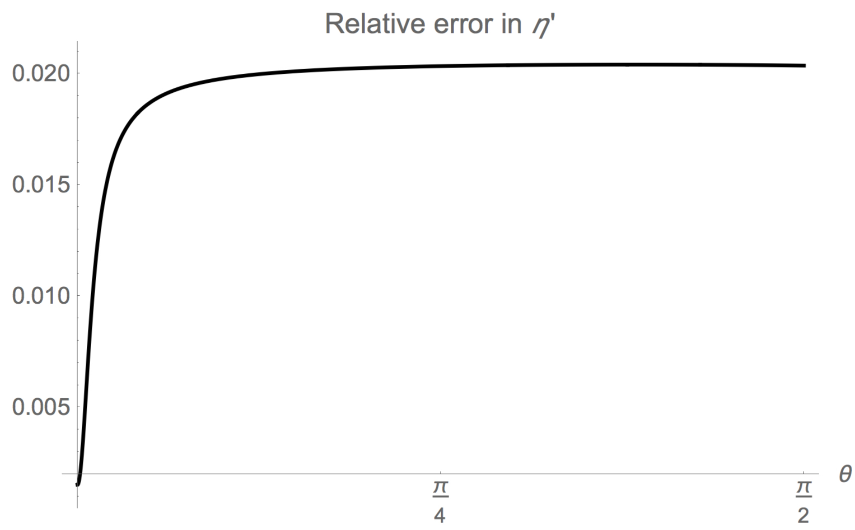

Figure 13. Relative error between $O(\mu^2)$ approximation to velocity, $\eta'(\theta)$ (using Equation (33)) and numerical solution of Equation (11). $\mu = 0.1$.

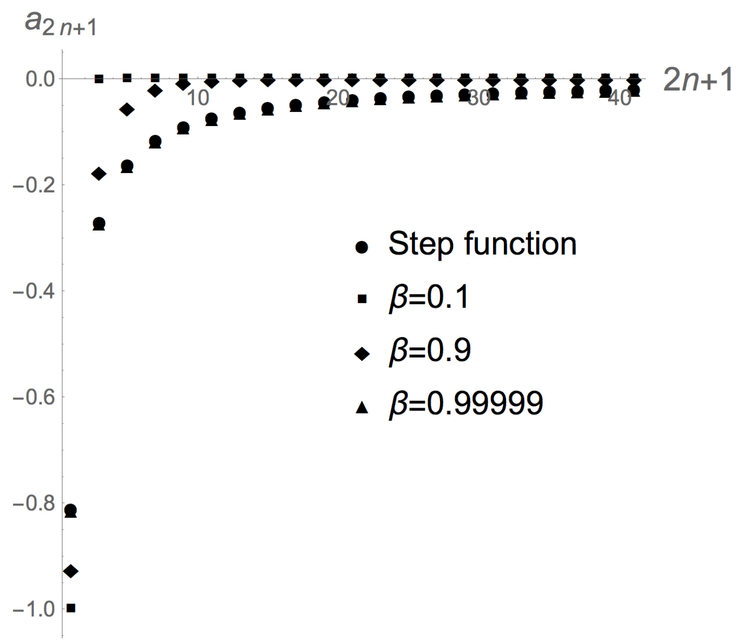

Figure 14. Fourier coefficients of $\eta'(\theta)$, from numerical solution of Equation (11), and spectrum of step-function Equation (35).

asymptotic step-function profile. For small β, the spectrum is dominated by a small number of modes. For $\beta \to 0$, the spectrum tends to a single mode, $\sin(\theta)$. The analysis in Section 4 exhibits the β—dependence of the modes for small β: $\sin((2n+1)\theta)$ modes appear in $O(\beta^{2n})$. As β approaches 1, the Fourier coefficients tend to the limiting spectrum, which is $O(1)$ in μ.

6.2. Test of Quality of Approximate Solution in Extreme-Relativistic Limit

In Figure 15, a comparison between the Fourier coefficients of $\eta'(\theta)$, computed

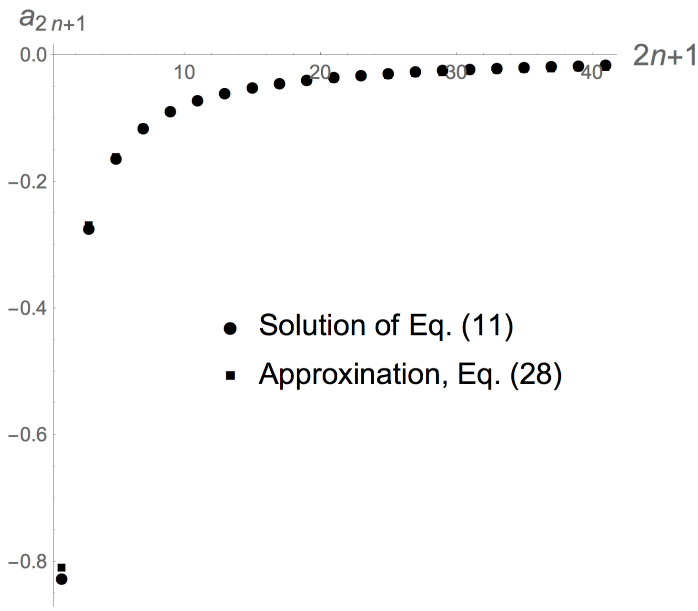

Figure 15. Fourier coefficients of $\eta(\theta)$ for approximate solution, Equations (28) and (32) and from numerical solution of Equation (11). $\mu = 0.2$.

for the approximate solution, Equations (28) and (32), with those obtained from the numerical solution of Equation (11) for $\mu = 0.2$ ($\beta = 0.992$) is presented for $1 \le 2n+1 \le 41$. The relative error between the exact numerical and the approximate values is below 5% for $1 \le 2n+1 \le 13$. For $\mu = 0.1$, the error is smaller than 0.5% for all $1 \le 2n+1 \le 41$.

7. Concluding Comments

The dynamics of the Relativistic Harmonic Oscillator (RHO) have been analyzed in the weak- and extreme-relativistic limits. Exploiting the fact that the period of oscillations can be computed in closed form and to any desired level of numerical accuracy, and using the scaled variables of Equation (10), for $\beta < 1$, a Normal Forms expansion yields a high quality approximation to the solution that is by far better than the standard application of asymptotic expansion methods.

The same formulation allows for the analysis of the extreme-relativistic limit as a boundary-layer problem, leading to a high-quality approximation for the solution for all $0 \le \theta \le (2\pi)$ for $(1-\beta) << 1$.

Statements and Declarations

The author declares that no funds, grants, or other support were received during the preparation of this manuscript.

The author has no relevant financial or non-financial interests to disclose.

1) The author made all contributions to the conception or design of the work. No data acquisition was required. No new software was created;

2) The author drafted the work or revised it critically for important intellectual content;

3) The author approved the version to be published; and

4) The author agrees to be accountable for all aspects of the work in ensuring that questions related to the accuracy or integrity of any part of the work are appropriately investigated and resolved.

Data Availability Statement

Data sharing is not applicable to this article, as no datasets were generated or analyzed during the current study.

Conflicts of Interest

The author declares no conflicts of interest regarding the publication of this paper.

References

[1] Bijtebier, J. (1977) On the Relativistic Harmonic Oscillator Quark Model for Baryons. *Bulletins de l'Académie Royale de Belgique*, **63**, 607-619. https://doi.org/10.3406/barb.1977.58271

[2] Ishida, S. and Sonoda, T. (1983) Relativistic Harmonic Oscillator Quark Model with Unequal Quark Masses. *Progress of Theoretical Physics*, **70**, 1323-1330. https://doi.org/10.1143/PTP.70.1323

[3] Bijtebier, J. (1984) The Relativistic Harmonic Oscillator Quark Model for Baryons as a Set of Coupled Klein-Gordon Equations. *Il Nuovo Cimento A*, **81**, 423-439. https://doi.org/10.1007/BF02724525

[4] Bannur, V.M. (2009) Relativistic Harmonic Oscillator Model for Quark Stars. *Modern Physics Letters A*, **24**, 3183-3191. https://doi.org/10.1142/S0217732309031272

[5] Cook, P.A. (1971) Relativistic Harmonic Oscillators with Intrinsic Spin Structure. *Lettere al Nuovo Cimento*, **1**, 419-426. https://doi.org/10.1007/BF02785170

[6] Bermudez, A., Martin-Delgado, M.A. and Solano, E. (2007) Exact Mapping of the 2 + 1 Dirac Oscillator onto the Jaynes-Cummings Model: Ion-Trap Experimental Proposal. *Physical Review A*, **76**, Article ID: 041801. https://doi.org/10.1103/PhysRevA.76.041801

[7] Martínez-y-Romero, R.P., Nunez-Yepez, H.N. and Salas-Brito, A.L. (1995) Relativistic Quantum Mechanics of a Dirac Oscillator. *European Journal of Physics*, **16**, 135-141. https://doi.org/10.1088/0143-0807/16/3/008

[8] Longhi, S. (2011) Classical Simulation of Relativistic Quantum Mechanics in Periodic Optical Structures. *Applied Physics B*, **104**, 453-468. https://doi.org/10.1007/s00340-011-4628-7

[9] Gerritsma, R., *et al.* (2010) Quantum Simulation of the Dirac Equation. *Nature*, **463**, 68-71. https://doi.org/10.1038/nature08688

[10] Gerritsma, R., *et al.* (2011) Quantum Simulation of the Klein Paradox with Trapped Ions. *Physical Review Letters*, **106**, Article ID: 060503. https://doi.org/10.1103/PhysRevLett.106.060503

[11] Castro, L.B. and Obispo, A.E. (2017) Generalized Relativistic Harmonic Oscillator in Minimal Length Quantum Mechanics. *Journal of Physics A*: *Mathematical and Theoretical*, **50**, Article ID: 285202. https://doi.org/10.1088/1751-8121/aa70f1

[12] Godoy, S. (2022) Dirac Quantum Beats in Extreme Relativistic Diffraction in Time.

Journal of Applied Mathematics and Physics, **10**, 1711-1720.
https://doi.org/10.4236/jamp.2022.105119

[13] Longhi, S. (2010) Photonic Realization of the Relativistic Dirac Oscillator. *Optics Letters*, **35**, 1302-1304. https://doi.org/10.1364/OL.35.001302

[14] Franco-Villafañe, J.A., *et al.* (2013) First Experimental Realization of the Dirac Oscillator. *Physical Review Letters*, **111**, Article ID: 170405.
https://doi.org/10.1103/PhysRevLett.111.170405

[15] Hughston, L.P. (1982) The Relativistic Oscillator. *Proceedings of the Royal Society of London*, **383**, 459-466. https://doi.org/10.1098/rspa.1982.0112

[16] Moshinsky, M. and Szczepaniak, A. (1989) The Relativistic Oscillator. *Journal of Physics A*: *Mathematical and General*, **22**, L817-L819.
https://doi.org/10.1088/0305-4470/22/17/002

[17] Li, Z.F., *et al.* (2005) Relativistic Harmonic Oscillator. *Journal of Mathematical Physics*, **46**, Article ID: 103514. https://doi.org/10.1063/1.2054648

[18] Bars, I. (2009) Relativistic Harmonic Oscillator Revisited. *Physical Review D*, **79**, Article ID: 045009. https://doi.org/10.1103/PhysRevD.79.045009

[19] Poszwa, A. (2014) Relativistic Generalizations of the Quantum Harmonic Oscillator. *Acta Physica Polonica A*, **226**, 1226-1234.
https://doi.org/10.12693/APhysPolA.126.1226

[20] Chargui, Y., Abdel-Rahman, K. and Abdel-Ilah, F. (2021) The Generalized Relativistic Harmonic Oscillator with a Point Interaction. *Heliyon*, **7**, e08628.
https://doi.org/10.1016/j.heliyon.2021.e08628

[21] Nagiyev, S.N. and Mir-Kasimov, R.M. (2021) Relativistic Linear Oscillator Unser the Action of a Constant External Force. Wave Functions and Dynamical Symmetry Groups. *Theoretical and Mathematical Physics*, **208**, 1265-1276.
https://doi.org/10.1134/S0040577921090087

[22] Clemnov, P.C. and Willson, A.J. (1956) The Dispersion Equation in Plasma Oscillations. *Proceedings of the Royal Society A*, **237**, 117-131.
https://doi.org/10.1098/rspa.1956.0165

[23] Buti, B. (1963) Relativistic Effects of Plasma Oscillation and Two-Stream Instability. I. *The Physics of Fluids*, **6**, 89-99. https://doi.org/10.1063/1.1724513

[24] Chizhonkov, E.V., Frolov, A.A. and Gorbunov, L.M. (2008) Modelling of Relativistic Cylindrical Oscillations in Plasma. *Russian Journal of Numerical Analysis and Mathematical Modelling*, **23**, 455-467. https://doi.org/10.1515/RJNAMM.2008.026

[25] Schroeder, C.B. (2009) Warm Plasma Model of Intense, Short-Pulse Laser-Plasma Interactions. *Journal of Physics*: *Conference Series*, **169**, Article ID: 012007.
https://doi.org/10.1088/1742-6596/169/1/012007

[26] Chizhonkov, E.V. and Frolov, A.A. (2011) Numerical Simulation of the Breaking Effect in Nonlinear Axially-Symmetric Plasma Oscillations. *Russian Journal of Numerical Analysis and Mathematical Modelling*, **26**, 379-396.
https://doi.org/10.1515/rjnamm.2011.021

[27] Maity, C., Chakrabarti, N. and Sengupta, S. (2011) Relativistic Effects on Nonlinear Lower Hybrid Oscillations in Cold Plasma. *Journal of Mathematical Physics*, **52**, Article ID: 043101. https://doi.org/10.1063/1.3574354

[28] Marinelli, A., Hemsing, E. and Rosenzweig, B. (2012) Three-Dimensional Analysis of Longitudinal Plasma Oscillations in a Thermal Relativistic Electron Beam: Application to an Initial Value Problem. *Physics of Plasmas*, **19**, Article ID: 063108.
https://doi.org/10.1063/1.4714639

[29] Chizhonkov, E.V. (2017) Diagnostics of a Gradient Catastrophe for a Class of Quasilinear Hyperbolic Systems. *Russian Journal of Numerical Analysis and Mathematical Modelling*, **32**, 13-26. https://doi.org/10.1515/rnam-2017-0002

[30] Frolov, A.A. and Chizhonkov, E.V. (2017) Breaking of Two-Dimensional Relativistic Electron Oscillations under Small Deviations from Axial Symmetry. *Computational Mathematics and Mathematical Physics*, **57**, 1808-1821. https://doi.org/10.1134/S0965542517110069

[31] Karmakar, M., Maity, C. and Chakrabarti, N. (2018) Relativistic Electron Plasma Oscillations in an Inhomogeneous Ion Background. *Physica Scripta*, **93**, Article ID: 065601. https://doi.org/10.1088/1402-4896/aac396

[32] Chizhonkov, E.V. and Frolov, A.A. (2019) Influence of Electron Temperature on Breaking of Plasma Oscillations. *Russian Journal of Numerical Analysis and Mathematical Modelling*, **34**, 71-84. https://doi.org/10.1515/rnam-2019-0006

[33] De Parga, G.A. and García-Camacho, J.F. (2019) Modified Vlasov Equation and Collective Oscillations of Relativistic Radiating Electron Plasma. *Journal of Physics: Conference Series*, **1239**, Article ID: 012001. https://doi.org/10.1088/1742-6596/1239/1/012001

[34] Frolov, A.A. and Chizhonkov, E.V. (2020) On the criteria of the Langmuir oscillations breaking in a Plasma. *Physica Scripta*, **95**, Article ID: 065604. https://doi.org/10.1088/1402-4896/ab85fe

[35] Frolov, A.A. and Chizhonkov, E.V. (2020) Application of the Energy Conservation Law in the Cold Plasma Model. *Computational Mathematics and Mathematical Physics*, **60**, 498-513. https://doi.org/10.1134/S0965542520030094

[36] Rozanova, O.S. and Chizhonkov, E.V. (2020) On the Existence of a Global Solution of a Hyperbolic Problem. *Doklady Mathematics*, **101**, 254-256. https://doi.org/10.1134/S1064562420030163

[37] Ashkenazy, Y., Goren, C. and Horwitz, L.P. (1998) Chaos of the Relativistic Parametrically Forced van der Pol Oscillator. *Physics Letters A*, **243**, 195-204. https://doi.org/10.1016/S0375-9601(98)00240-0

[38] Babusci, D., *et al.* (2013) Relativistic Harmonic Oscillator, the Associated Equations of Motion, and Algebraic Integration Methods. *Physical Review E*, **87**, Article ID: 033202. https://doi.org/10.1103/PhysRevE.87.033202

[39] Browaeys, A., *et al.* (2005) Transport of Atoms in a Quantum Conveyor Belt. *Physical Review A*, **72**, Article ID: 053605. https://doi.org/10.1103/PhysRevA.72.053605

[40] Grossert, C., Leder, M. and Weitz, M. (2016) Phase Dependent Loading of Bloch Bands and Quantum Simulation of Relativistic Wave Equation Predictions with Ultracold Atoms in Variably Shaped Optical Lattice Potentials. *Journal of Modern Optics*, **63**, 1805-1813. https://doi.org/10.1080/09500340.2015.1137370

[41] Fujiwara, K.M., *et al.* (2018) Experimental Realization of a Relativistic Harmonic Oscillator. *New Journal of Physics*, **20**, Article ID: 063027. https://doi.org/10.1088/1367-2630/aacb5a

[42] Penfield, R. and Zatzkis, H. (1956) The Relativistic Linear Harmonic Oscillator. *Journal of the Franklin Institute*, **262**, 121-125. https://doi.org/10.1016/0016-0032(56)90762-1

[43] MacColl, L.A. (1957) Theory of the Relativistic Oscillator. *American Journal of Physics*, **25**, 535-539. https://doi.org/10.1119/1.1934543

[44] Taylor, N.W. (1961) Note on the Harmonic Oscillator in General Relativity. *Journal of the Australian Mathematical Society*, **2**, 206-208.

https://doi.org/10.1017/S1446788700026677

[45] Mithchell, T.P. and Pope, D.L. (1962) On the Relativistic Damped Oscillator. *Journal of the Society for Industrial and Applied Mathematics*, **10**, 49-61. https://doi.org/10.1137/0110005

[46] Hutten, E.H. (1965) Light Scattering by the Relativistic (Non-Linear) Oscillator. *Nature*, **207**, Article 854. https://doi.org/10.1038/207854a0

[47] Mickens, R.E. (1998) Periodic Solutions of the Relativistic Harmonic Oscillator. *Journal of Sound & Vibration*, **212**, 905-908. https://doi.org/10.1006/jsvi.1997.1453

[48] Beléndez, A. and Pascual, C. (2007) Harmonic Balance Approach to the Periodic Solutions of the (an)Harmonic Relativistic Oscillator. *Physics Letters A*, **371**, 291-299. https://doi.org/10.1016/j.physleta.2007.09.010

[49] Beléndez, A., *et al.* (2008) Higher-Order Approximate Solutions to the Relativistic and Duffing Oscillators by Modified He's Homotopy Method. *Physica Scripta*, **77**, Article ID: 025004.https://doi.org/10.1088/0031-8949/77/02/025004

[50] Biazar, J. and Hosami, M. (2014) An Easy Trick to a Periodic Solution of Relativistic Harmonic Oscillator. *Journal of the Egyptian Mathematical Society*, **22**, 45-49. https://doi.org/10.1016/j.joems.2013.04.013

[51] Harvey, A.L. (1972) Relativistic Harmonic Oscillator. *Physical Review D*, **6**, 1474-1476. https://doi.org/10.1103/PhysRevD.6.1474

[52] Moreau, W., Easther, R. and Neutze, R. (1994) Light Scattering by the Relativistic (Non-Linear) Oscillator. *American Journal of Physics*, **62**, 531-535. https://doi.org/10.1119/1.17513

[53] Huang, Y.S. (1999) An Alternative Derivation of the Equations of Motion of the Relativistic (an)Harmonic Oscillator. *American Journal of Physics*, **67**, 142-145. https://doi.org/10.1119/1.19209

[54] Chakraborty, P. (2015) Relativistic Harmonic Oscillator. *Scholars Journal of Physics, Mathematics and Statistics*, **2**, 349-352.

[55] De la Fuente, D. and Torres, P.J. (2017) A New Relativistic Extension of the Harmonic Oscillator Satisfying an Isochronicity Principle. *Qualitative Theory of Dynamical Systems*, **16**, 579-589. https://doi.org/10.1007/s12346-016-0207-y

[56] Parker, E. (2017) A Relativistic Gravity Train. *General Relativity and Gravitation*, **49**, Article No. 106. https://doi.org/10.1007/s10714-017-2267-y

[57] Anderson, R.L. (2020) Non-Covariant Lagrangians Are Presented, Which Yield Two-Component Equations of Motion for a Class of Relativistic Mechanical Systems in 1 + 1 Dimensions Including the Harmonic Oscillator. *Applied Mathematics*, **11**, 917-921. https://doi.org/10.4236/am.2020.119059

[58] Poincaré, H. (1892) Les Methods Nouvelles de la Mécanique Célest, t. 1 (Gauthier-Villars, Paris, 1892) (Dover, New York, 1957).

[59] Lie, S. (1888) Theorie der Trasfomationgruppen I. *Mathematische Annalen*, **16**, 441-528.

[60] Birkhoff, G.D. (1927) Dynamical Systems. American Mathematical Society. American Mathematical Society, New York. https://doi.org/10.1090/coll/009

[61] Hori, G.I. (1971) Theory of General Perturbations for Non-Canonical Systems. *Publications of the Astronomical Society of Japan*, **23**, 567-587.

[62] Arnold, V.I. (1988) Geometrical Methods in the Theory of Differential Equations. Springer, New York. https://doi.org/10.1007/978-3-662-11832-0

[63] Bruno, A.D. (1989) Local Methods in Nonlinear Differential Equations. Springer,

Berlin. https://doi.org/10.1007/978-3-642-61314-2

[64] Guckenheimer, J. and Holmes, P. (1983) Nonlinear Oscillations, Dynamical Systems and Bifurcations. Springer, New York. https://doi.org/10.1007/978-1-4612-1140-2

[65] Kahn, P.B. and Zarmi, Y. (1998) Nonlinear Dynamics: Exploration through Normal Forms. Wiley, New York.

[66] Murdock, J. (2003) Normal Forms and Unfoldings for Local Dynamical Systems. Springer, New York. https://doi.org/10.1007/b97515

[67] Gradshteyn, I.S. and Ryzhik, I.M. (2007) Tables of Integrals, Series and Products. 7th Edition, Elsevier, Amsterdam.